Int J Ind Chem (2014) 5:18
DOI 10.1007/s40090-014-0018-4

RESEARCH

Characterization of cerate–zirconate ceramic powder prepared by a high-pressure–high-temperature batch-wise reactor system

Najwa 'Adni Ibarahim · Mohd Azlan Mohd Ishak · Azliana Ramli · Nafisah Osman

Received: 12 November 2013 / Accepted: 21 June 2014 / Published online: 12 July 2014

Abstract A supercritical technique was proposed to synthesise cerate–zirconate ceramic compound by a high-pressure–high-temperature batch-wise reactor system. TG thermogram of the dried powders for all samples showed three stages of weight loss. Each stage is corroborated by one or two exothermic peaks as shown in DTG signal. A complete thermal decomposition for all samples is accomplished at ~977 °C for 2 h. FT-IR and XRD patterns showed the traces of carbonate residue in the calcined samples is due to the incomplete combustion of intermediate compounds. The presence of secondary phases, namely, $BaZrO_3$, $BaCeO_3$, BaO_2 and CeO_2 as detected by XRD measurement indicates that the calcined samples are not in a single phase of cerate–zirconate compound.

Keywords Ceramic perovskite-type oxides · Supercritical fluids · Phase formation

Introduction

Protonic conductors of ceramic perovskite-type oxides (ABO_3) have captured attention of researchers worldwide for technological purpose in fuel cells, batteries, steam electrolyser, etc. The best candidate amongst them is the perovskite-type oxides of $Ba(Ce,Zr)O_3$ which is known to exhibit high mechanical and chemical stability along with good conductivity. This proton conductor is the best applicant as electrolyte for solid oxide fuel cells (SOFC) in the presence of hydrogen and/or water vapour at intermediate temperatures (400–750 °C) [1, 2].

Conventionally, the ceramic electrolytes have been prepared by solid-state reaction (SSR) method which employed ball-milled, repetitive grinding and high-temperature treatment ($T > 1{,}400$ °C). As a consequence, some impurities contaminations were introduced through the heat treatment process which cause sample degradation. To overcome the SSR shortcomings, wet chemical methods (WCMs) such as sol–gel, hydrothermal, co-precipitation, etc. [3–5], are adopted to obtain the desired perovskite compound. WCMs offer fine powder morphologies with less contamination. However, this technique requires longer time and high-temperature treatment ($T > 1{,}250$ °C) to eliminate organic residues such as carbonate species; thus leads to high energy costs.

Recently, green chemistry technology introduces supercritical fluids (SCF) as one of the promising techniques in synthesising perovskite-type oxide materials. The unique properties of the SCF are the adjustment of its operating conditions as well as physical and chemical parameters (pressure, temperature, and organic solvent) which are difficult to obtain or adjust with conventional processes. The advantages of the SCF are it is a highly versatile technique in producing nano-sized powder and helps to minimise the release of carbon dioxide gas in atmosphere that contributes to massive greenhouse effect and global warming.

The widely used solvents in SCF synthesis as reported in literature are CO_2, H_2O, CO_2 with alcohol, and alcohol [6, 7]. Low carbon alcohols are frequently being used as

N. 'AdniIbarahim (✉) · M. A. M. Ishak · A. Ramli · N. Osman
Faculty of Applied Sciences, Universiti Teknologi MARA, 02600 Arau, Perlis, Malaysia
e-mail: najwaadni88@yahoo.com

N. Osman
e-mail: fisha@perlis.uitm.edu.my

N. 'AdniIbarahim
Faculty of Applied Sciences, Universiti Teknologi MARA, 40450 Shah Alam, Selangor, Malaysia

solvent because they can act both as solvent and a reducing agent at supercritical condition [8]. In this present work, a high-pressure–high-temperature (HP-HT) batch-wise reactor system was used to synthesise $BaCe_{0.54}Zr_{0.36}Y_{0.1}O_{2.95}$ (BCZY) perovskite powder using ethanol as SCF media.

Experimental procedure

Sample preparation

$Ba(NO_3)_2$(99 %, ACROS), $Ce(NO_3)_3{\cdot}6H_2O$ (99.5 %, ACROS), $Zr(NO_3)_2O{\cdot}xH_2O$ (99.5 %, ACROS) and $Y(NO_3)_3{\cdot}5H_2O$ (99.9 %, Aldrich) were used as starting or precursor materials. Ethanol (95 %, HmbG) was used as solvent and reaction media. Each metal nitrate salt in stoichiometric amount was dissolved in ethanol. The mixture of the precursor materials was loaded inside a 350-mL vessel and synthesised by a HP-HT batch-wise reactor system. The temperature and pressure of the solvent were controlled at various conditions using a controller as shown in Table 1. The amount of solvent depends on the percentage of liquid level filling or percent of reactor-free volume as reported by Ishak [9]. The facilities involved in monitoring the parameters are flow meters, temperature controller (thermocouple type-K located inside the vessel) and a back-pressure regulator (Unijin). After a fixed period of time, the vessel was transferred into a water bath to quench the reaction immediately. The obtained slurry was subjected to a vacuum suction to separate solid from the slurry. Rotary evaporator was used to evaporate the remaining solvent and the solid product was further calcined at 1,100 °C at a heating rate of 10 °C/min.

Sample characterization

The thermal decomposition process for the as-synthesised dried BCZY powders was analysed by thermogravimetric analyzer/differential scanning calorimeter (TGA/DSC) (TA Instrument, SDT Q600). Approximately 15–18 mg of the dried powder was placed in an alumina crucible pan and gradually heated from 25 to 1,000 °C with heating rate of 10 °C/min under purified air. The infrared spectroscopy analysis was performed at room temperature using FT-IR Nicolet 380 spectrophotometer. The IR spectrum was used to observe the formation of metal oxide and detect the remaining carbonate ions of the as-synthesised and calcined powders from 400 to 4,000 cm^{-1}. The phase identification of the samples was carried out by X-ray diffractometer (Shimadzu XRD-6000) equipped with Ni-filtered and graphite monochromatized Cu-K_α radiation ($\lambda = 1.5406$ Å) over a 2θ range of 10°–80° with step size at 0.02°/s.

Table 1 Denomination of BCZY sample at different pressures and temperatures

Denomination	Pressure (MPa)	Temperature (°C)
S4	4	200
S8	8	200
C6	7	250
P4	4	300
P8	8	300

Results and discussion

Thermogravimetric analysis

The TG–DTG thermograms of the dried powder ($T = 250$ °C) of BCZY are shown in Fig. 1. All of the samples exhibit almost similar pattern of TG/DTG profiles which consists of three stages of weight loss. Stage 1 takes place in the range of 26–150 °C with the weight loss of about ~2–4 % corresponding to the evaporation of residual water (H_2O) and/or moisture. The second stage at ~150–480 °C with the weight loss of about 7–14 % is associated with the removal of residual water/moisture, ethanol and decomposition of organic complexes such as nitrate ions. A work done by Ru et al. [10] also suggested that the volatilization of excess ethanol can be seen at the same range as being observed in this work.

Stage 3 at 400–977 °C shows the largest weight loss of about 16–21 %. It can be devoted to the release of organic residues such as CO, CO_2 and NO_x gasses [11]. At this stage, the decomposition of carbonaceous residues gives rise to the formation of oxide compounds with the release of CO_2. There is no apparent change in the weight loss observed when the temperature is higher than 1,000 °C, indicating that the decomposition of $BaCO_3$ and the formation of BCZY may occur. Therefore, it is expected that the minimum temperature of 1,000 °C is needed to calcine the dried powders.

The possible step-by-step process of weight loss for all samples can be explained as follows:

Step A:

- Boiling point of ethanol (C_2H_6O) → 78 °C
- Boiling point of H_2O → 100 °C

Step B:

- Vapourization of organic complexes obtained from polymerized complex reaction of metal nitrate [10].
- EtOH ↔ ethene + H_2O
- Combustion of residual alcohol
- $C_2H_5OH(liq) + 3O_2(g) \rightarrow 2CO_2(g) + 3H_2O\ (g)$

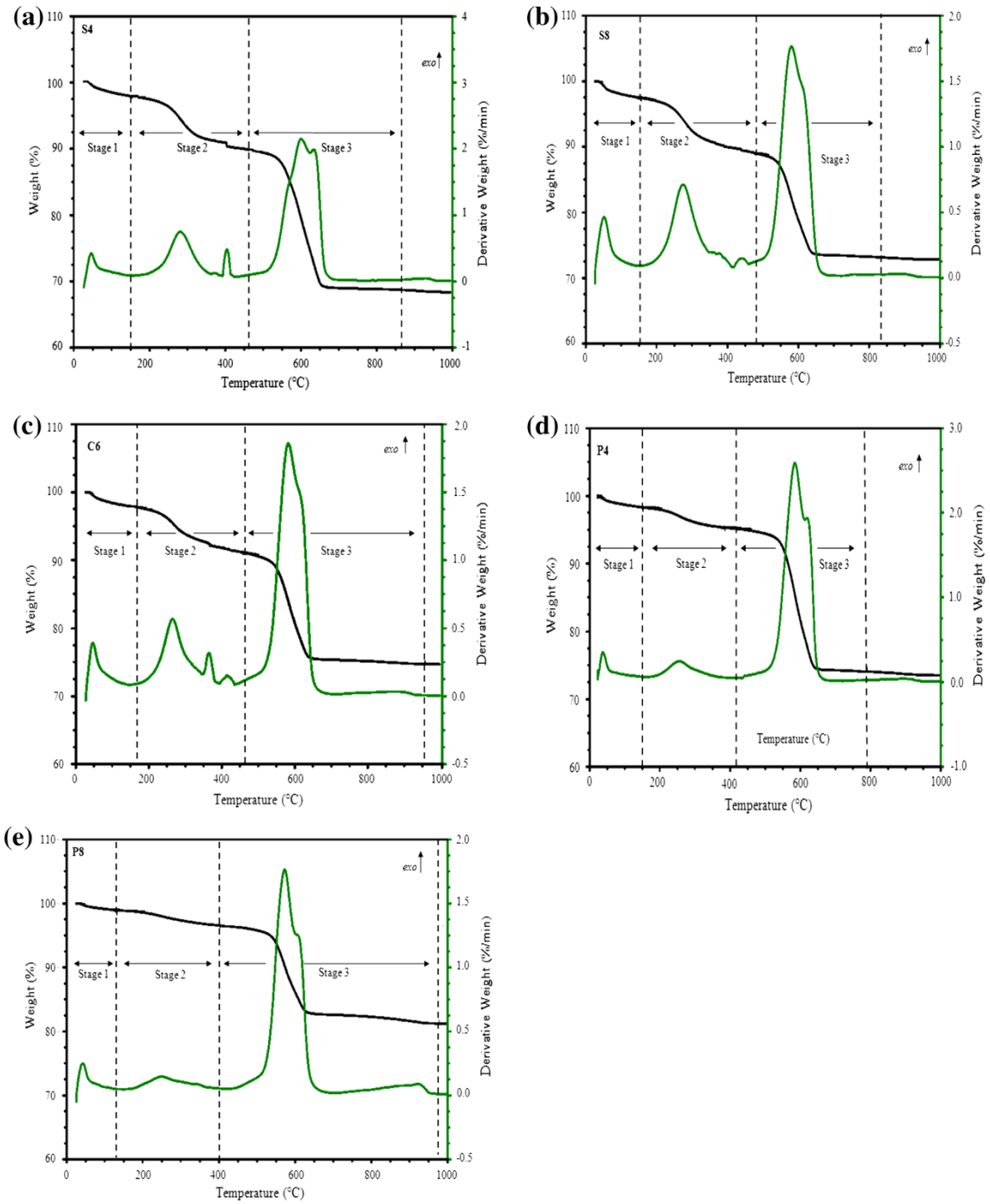

Fig. 1 TG/DTG thermograms of the dried BCZY powders. **a** S4, **b** S8, **c** C6, **d** P4 and **e** P8 at different pressures and temperatures

Step C:

- $BaCO_3 + Ce_{1-x}Zr_xO_2 \rightarrow BaCe_{1-x}Zr_xO_3 + CO_2$

[12].

A summary of weight loss for all samples is presented in Table 2.

Fourier transform infrared spectroscopy (FT-IR)

The bonding characteristics of functional groups for the as-synthesised and calcined powders were identified by FT-IR spectroscopy as shown in Fig. 2. For the as-synthesised powders, a small absorption band around

Table 2 Weight loss for dried BCZY powder ($T = 250$ °C)

Sample	Stage	Temperature range (°C)	Weight loss (%)	Total weight loss (%)
S4	1	30–150	2	31
	2	150–470	8	
	3	470–860	21	
S8	1	26–150	3	28
	2	150–480	9	
	3	480–830	16	
C6	1	26–166	2	25
	2	166–470	7	
	3	470–950	16	
P4	1	25–160	2	26
	2	160–420	3	
	3	420–830	21	
P8	1	26–130	2	20
	2	130–400	2	
	3	400–977	16	

1,622 cm^{-1} for P8 is characteristic of absorbed water or hydroxyl group (O–H stretching) in ethanol. Broad peak around 1,580–1,552 cm^{-1} is attributed to bidentate carbonates and/or carboxylate ion. The characteristics of metal precursors bound to nitrate group (M-NO_3) for all samples are shown by two absorption peaks that appeared at ~1,421–1,415 and 1,380–1,358 cm^{-1}, respectively [13]. The presence of a small sharp peak at 816–808 cm^{-1} indicates that the samples consist of carbonate species as secondary phases due to decomposition of metal nitrate with CO_2. The formation of metal–oxygen (M–O) bond in the prepared sample is represented by small sharp peak at 729–720 cm^{-1} for S4, S8 and C6 which is in-line with the work done by Li et al. [14]. The presence of metal oxides is noticeable for S4, S8, and P8 by the appearance of broad adsorption bands at 542–466 cm^{-1}.

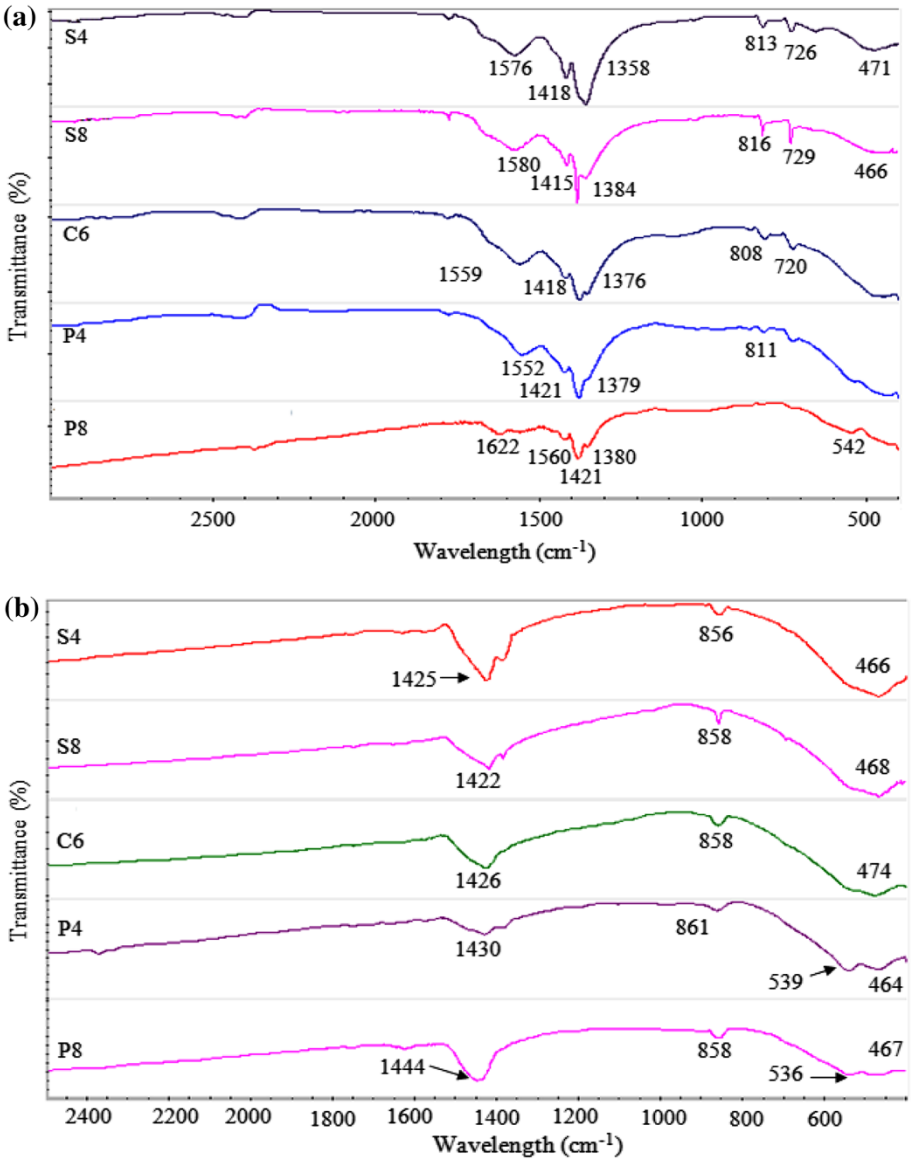

Fig. 2 FT-IR spectra of BCZY powders. **a** As-synthesised. **b** After calcined at $T = 1{,}100$ °C

In Fig. 2b, as calcination temperature is increased to 1,100 °C, the bands associated to the -OH and other organic compounds vibration became weaker and the bands for the metal–oxygen vibration became stronger. However, the presence of impurities such as nitrate species at ~1,444–1,422 cm^{-1} [15] and carbonate residue at 861–856 cm^{-1} are still being detected in the spectra. Carbonate compound was formed due to the incomplete combustion of excessive organic matter with $Ba(NO)_2$ [13]. According to Robertz et al. and Osman et al., high calcination temperatures ranging from 1,400 to 1,500 °C are needed to decompose the carbonate traces and undesired secondary phases [12, 16]. The broad absorption bands between 539 and 464 cm^{-1} indicate the presence of metal oxides in the samples.

X-ray diffraction (XRD)

Figure 3 shows XRD patterns of the prepared powders after they were calcined at 1,100 °C. All samples exhibit a mixture of respective $BaZrO_3$, $BaCeO_3$, CeO_2, BaO_2 and $BaCO_3$. For example, peak at $2\theta = 28.5°$ is corresponded to the $BaCeO_3$ (JCPDS card- 220,074) and at $2\theta = 30°$ for $BaZrO_3$ (JCPDS card- 60039). The SCF condition used in this work also produces CeO_2 and BaO_2, which are initial compounds to form $BaCeO_3$. Detailed literature survey showed that single metal oxides or/and perovskite phase can be obtained if the sample has only 2–3 metal elements such as $BaTiO_3$, TiO_2, and ZrO_2 [8, 17, 18]. For the sample consisting of four metal elements, the conditions used in SCF are not suitable and sufficient enough to produce a single perovskite of $Ba(Ce,Zr)O_3$. On the other hand, the formation of $BaCO_3$ is due to the reaction between Ba^{2+} and CO_3^{2-} during the calcination process. Therefore, further modification technique using a supercritical fluid that assisted with sol–gel method to produce a single BCZY phase will be applied in our future work.

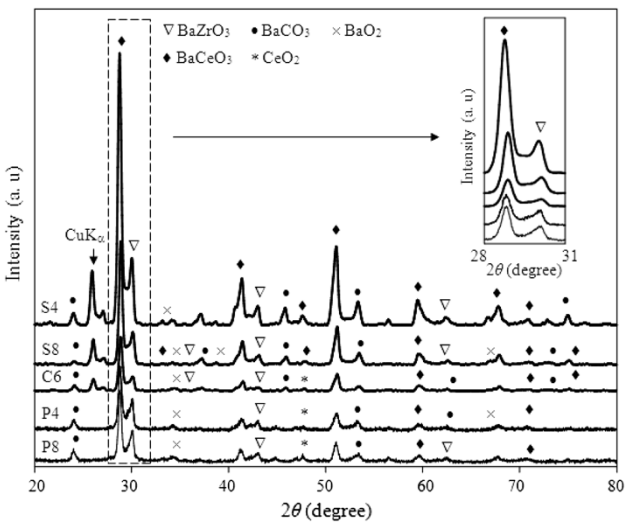

Fig. 3 XRD patterns for prepared powder after calcined at 1,100 °C

Conclusion

A precursor of metal nitrate salts in stoichiometric amount was synthesised by a supercritical ethanol at different pressures and temperatures. The dried powder was decomposed at ~977 °C based on TG–DTG results. The analyses of FT-IR and XRD data clearly revealed that the prepared sample consists of carbonate species and secondary phase mainly individual perovskite of $BaCeO_3$, $BaZrO_3$, and metal oxides, respectively. The parameters of ScEtOH, particularly pressure and solubility were not desirable enough to bind the metal elements and hindered the formation of carbonate species at an early state. Consequently, the incomplete reaction produces $BaCO_3$ and other secondary phases. Therefore, we conclude that the conditions used in SCF in this work were not sufficient to substitute Ce into Zr site to form a single phase of cerate–zirconate compound. Modification on the synthesis route is still in progress and will be reported elsewhere.

Acknowledgments The authors would like to thank the Ministry of Education (MOE), Malaysia for the Research Articulation Grant Scheme (RAGS), Exploratory Research Grant Scheme (ERGS) and Universiti Teknologi MARA for the internal grant and facilities support.

References

1. Katahira K, Kohchi Y, Shimura T, Iwahara H (2000) Protonic conduction in Zr-substituted $BaCeO_3$. Solid State Ion 138:91–98
2. Babilo P, Haile SM (2005) Enhanced sintering of yttrium-doped Barium Zirconate by addition of ZnO. J Am Ceram Soc 88:2362–2368
3. Osman N, Talib IA, Hamid HA (2008) Properties of sol–gel prepared $BaCeO_3$ solid electrolyte using acetate precursors. Ionics 15:203–208
4. Amini MM, Mirzaee M (2009) Effect of solvent and temperature on the preparation of potassium niobate by hydrothermal-assisted sol–gel processing. Ceram Int 35:2367–2372
5. Boschini F, Rulmont A, Cloots R, Vertruyen B (2009) Rapid synthesis of submicron crystalline barium zirconate $BaZrO_3$ by precipitation in aqueous basic solution below 100 °C. J Eur Ceram Soc 29:1457–1462
6. Aymonier C, Serani LA, Reveron H, Garrabos Y, Cansell F (2006) Review of supercritical fluids in organic material science. J Supercrit Fluids 38:242–251
7. Aimable A, Xin B, Millot N, Aymes D (2008) Continuous hydrothermal synthesis of nanometric $BaZrO_3$ in supercritical water. J Solid State Chem 181:183–189

8. Kim J, Kim D, Veriansyah B, Kang JW, Kim J-D (2009) Metal nanoparticle synthesis using supercritical alcohol. Mater Lett 63:1880–1882
9. Ishak MAM (2007) A Study on liquefaction of pretreated mukah balingan low rank malaysia coal, Chapter 3: Materials and methods, 25
10. Ru Y, Jie Q, Min L, Guoqiang L (2008) Synthesis of yttrium aluminum garnet (YAG) powder by homogeneous precipitation combined with supercritical carbon dioxide or ethanol fluid drying. J Eur Ceram Soc 28:2903–2914
11. Singh KA, Pathak LC, Roy SK (2007) Effect of citric acid on the synthesis of nano-crystalline yttria stabilized zirconia powders by nitrate–citrate process. Ceram Int 33:1463–1468
12. Osman N, Talib IA, Hamid HA (2010) Preparation and characterization of Yb-doped $Ba(Ce,Zr)O_3$ nanopowders with high sinterability. Ionics 16:561–569
13. Nityanand C, Nalin WB, Rajkumar BS, Chandra CM (2011) Synthesis and physicochemical characterization of nanocrystalline cobalt doped lanthanum strontium ferrite. Solid State Sci 13:1022–1030
14. Li Y, Zhao J, Wang B (2004) Low temperature preparation of nanocrystalline $Sr_{0.5}Ba_{0.5}Nb_2O_6$ powders using an aqueous organic gel route. Mater Res Bull 39:365–374
15. Milt VG, Ulla MA, Miro EE (2005) NO_x trapping and soot combustion on $BaCoO_{3-y}$ perovskite: LRS and FTIR characterization. Appl Catal B 57:13–21
16. Robertz B, Boschini F, Rulmont A, Clossts R (2003) Preparation of $BaZrO_3$ powders by a spray-drying process. J Mater Res 18:1325–1332
17. Alonso E, Montequi I, Lucas S, Cocero MJ (2007) Synthesis of titanium oxide particles in supercritical CO_2: effect of operational variables in the characteristics of the final product. J Supercrit Fluids 39:453–461
18. Byrappa K, Ohara S, Adschiri T (2008) Nanoparticles synthesis using supercritical fluid technology—towards biomedical applications. Adv Drug Deliv Rev 60:299–327